Formation and stability of cubic ice in water droplets

Benjamin J. Murray and Allan K. Bertram*

Received 22nd September 2005, Accepted 13th October 2005
First published as an Advance Article on the web 2nd November 2005
DOI: 10.1039/b513480c

There is growing evidence that a metastable phase of ice, cubic ice, plays an important role in the Earth's troposphere and stratosphere. Cubic ice may also be important in diverse fields such as cryobiology and planetary sciences. Using X-ray diffraction, we studied the formation of cubic ice in pure water droplets suspended in an oil matrix as a function of droplet size. The results show that droplets of volume median diameter 5.6 μm froze dominantly to cubic ice with stacking faults. These results support previous suggestions that cubic ice is the crystalline phase that nucleates when pure water droplets freeze homogeneously at ~235 K. It is also shown that as the size of the water droplets increased from 5.6 to 17.0 μm, the formation of the stable phase of ice, hexagonal ice, was favoured. This size dependence can be rationalised with heat transfer calculations. We also investigated the stability of cubic ice that forms in water droplets suspended in an oil matrix. We observe cubic ice up to 243 K, much higher in temperature than observed in many previous studies. This result adds to the existing literature that shows bulk ice I_c can persist up to ~240 K. The transformation of cubic ice to hexagonal ice also showed a complex time and temperature dependence, proceeding rapidly at first and then slowing down and coming to a halt. These combined results help explain why cubic ice forms in some experiments described in the literature and not others.

Introduction

Recently, it was found that cubic ice (ice I_c), as opposed to the stable hexagonal phase (ice I_h), was the major product when aqueous solution droplets froze homogeneously at temperatures of less than 200 K.[1] This strongly suggests ice I_c forms in the Earth's upper troposphere where it may significantly impact the formation of ice clouds and enhance dehydration through a process analogous to the well known Bergeron–Findeisen process.[2] This process is driven by the vapour pressure difference between ice I_c and ice I_h, where the metastable phase necessarily has a larger vapour pressure than that of the stable phase.[2] Ice I_c may also be important in other areas such as cryobiology and planetary sciences.[3]

In our recent study on cubic ice we observed that a small amount of ice I_c was formed when emulsified pure water droplets (water droplets suspended in an oil matrix) homogeneously froze at ~235 K.[1] This was unexpected as prior to our work, ice I_c was only observed in pure water droplets when they were hyperquenched onto a cold substrate below 190 K.[4] Ice I_c has also been observed when water clusters (6.6–5.5 nm) froze at 200 K.[5] Others have suggested that crystallisation of water droplets begins with nuclei having a cubic structure even at temperatures well above 200 K.[5–9] Clearly, more work is required to understand the conditions that are required for the formation of ice I_c.

To explain our previous results and better understand the conditions at which cubic ice forms in pure water droplets we have carried out two sets of experiments: first, we have investigated the formation of cubic ice in emulsified water droplets as a function of droplet size. Second, we have investigated the stability of ice I_c that forms in these emulsified droplets. One of the benefits of our experimental configuration is that mass transfer *via* the vapour phase is blocked since the droplets are suspended in an oil matrix. This allows us to focus on the solid state transformation in contrast to many previous measurements. Our combined studies provide insight into the nucleation and crystallization process, and allow us to speculate on the structure of the crystalline nucleus responsible for homogeneous nucleation in water droplets, an important topic that still is not resolved. Our results, combined with previous results, also allow us to speculate why cubic ice forms in some experiments, which are recorded in the literature, and not in others.

Department of Chemistry, University of British Columbia, 2036 Main Mall, Vancouver, British Columbia, Canada V6T 1Z1

Experimental

The X-ray diffractometer (Bruker D8 Discover) employed in this study was configured in a standard Bragg–Brentano reflection geometry and was equipped with a Cu Kα X-ray source and a Bruker SOL-X X-ray detector. In order to improve the signal-to-noise a different source and detector to those described by Murray *et al.*[1] were employed in the present study. Other than a factor of two improvements in signal-to-noise, the diffraction patterns from the present and previous studies are directly comparable.

Emulsions of pure water droplets were prepared by mixing pure water (distilled water further purified with a Millipore system) with an oil phase in a proportion of 30–40% water in oil (by mass). The oil phase consisted of ~10 wt% of surfactant (lanolin, Aldrich Chemical Company) in

hydrocarbon oil (paraffin oil, Fisher Scientific, kinematic viscosity at 40 °C = 34.5 cSt). This mixture was then agitated for 5–10 min or until the droplets were of the desired size. Droplet size could be varied by adjusting the agitation time and the resulting droplet size distribution was determined by optical microscopy (see the insert in Fig. 2 for an example of a size distribution determined by this method).

The X-ray diffraction experiments were performed with a modified commercial low temperature X-ray diffraction chamber (Anton-Paar, TTK 450). The emulsions were placed in a cell consisting of an aluminium base and covered with a 30 μm thick film of Teflon to hold the emulsions in place and also prevent evaporation of the droplets. The temperatures of the cell and emulsion were measured with a thermistor (Pt-100) positioned within the aluminium base. This cell was placed in good thermal contact with a cryostat, which was cooled with a flow of liquid nitrogen and the required temperature set by use of a heater and temperature controller (Anton-Paar, TCU). This system allowed the temperature of the emulsion cell to be set to between 90 and 300 K (and to higher temperatures if the liquid nitrogen flow was stopped). The uncertainty in the temperature was ±1 K based on melting point measurements. The temperature of the cell could be ramped up or down at rates up to 30 K min^{-1}, where 10 K min^{-1} was the standard cooling rate in the freezing experiments. The cryostat and emulsion cell were positioned inside an airtight chamber which could either be evacuated or purged with a dry flow of N_2 in order to prevent frosting at low temperatures. Windows made of Capton in the walls of this chamber permitted X-ray radiation to pass into and out of the chamber.

Since the droplets were suspended in an oil matrix preferred orientation of the crystals after freezing was not expected. Also, the measured diffraction patterns were expected to be equivalent to a powder X-ray pattern, since there were between 10^6 and 10^8 individual frozen droplets exposed to the X-ray beam in a typical experiment. To test these assumptions, we compared the diffraction pattern of the frozen droplets after annealing, which results in pure hexagonal ice (see Fig. 1a), with patterns of hexagonal ice calculated using the POWDER CELL programme[10] using crystallographic data for hexagonal ice.[11] The measured peak intensities were in excellent agreement with the calculations, indicating preferred orientation was not an issue. If there was a preferred orientation, or not enough frozen droplets to approximate a powder, the peak intensities would not match the calculations.

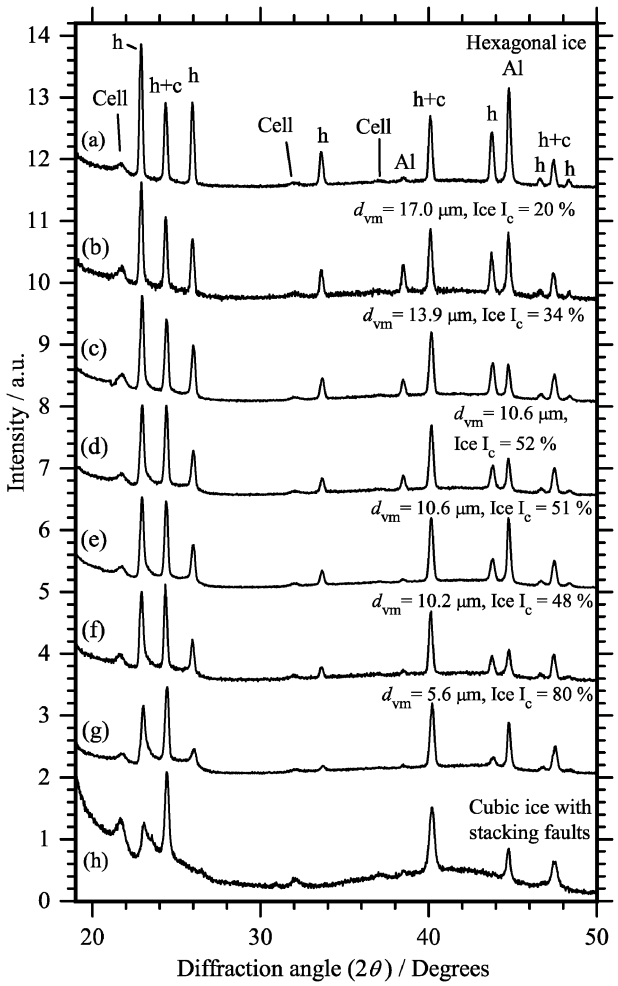

Fig. 1 Diffraction patterns of frozen droplets. Patterns (b) to (g) are the diffraction patterns of frozen pure water droplets, where the size of the droplets was varied. The volume median diameter, d_{vm}, is given for each pattern. The droplets were cooled at a rate of 10 K min^{-1} and froze between 237.5 ± 1 and 230.4 ± 1 K. The pattern shown in (a) is for the same frozen water droplets that appear in (f), but which were annealed at 263 K for 5 min to yield pure ice I_h. The diffraction pattern shown in (h) is a diffraction pattern of ice I_c with stacking faults. This pattern was obtained by freezing 45.2 wt% $(NH_4)_3H(SO_4)_2$ solution droplets, which froze between 192.4 ± 1 and 184.5 ± 1 K. The estimated proportion of stacking faulty ice I_c, determined from the linear combination of the hexagonal patterns (a) and cubic pattern (h), are given for patterns (b) to (g) (see text and Fig. 3 for details of this estimate). All patterns are normalized to the intensity of the peak at 40° and are shifted on the intensity scale for clarity. Reflections unique to ice I_h are labelled "h" and those common to ice I_c and ice I_h are labelled "h + c". Bragg peaks from the aluminium base and those from the cell construction materials are labelled Al and cell, respectively. All diffraction patterns were recorded at 173 K. The baseline in pattern (h) is more pronounced compared with the other patterns because of the smaller water content in the concentrated $(NH_4)_3H(SO_4)_2$ solution droplets.

Results and discussion

The formation of ice I_c in pure water droplets as a function of droplet size

Emulsions of pure water droplets were cooled to 173 K at a rate of 10 K min^{-1}, while monitoring a strong ice reflection (at either $2\theta \approx 24$ or 40°) in order to determine the freezing temperatures of the droplets. Freezing of droplets occurs over a range of temperatures, since nucleation is a stochastic process.[12] The observed freezing range of pure water droplets (between approximately 237.5 ± 1 and 230.4 ± 1 K) is in very good agreement with literature values for homogeneous freezing of micrometer sized droplets,[12] indicating that the oil and surfactant were not significantly altering the nucleation process and that these droplets froze homogeneously. The observed freezing range varied by less than the uncertainty in the

measurements as the volume median diameter varied from 5.6–17.0 μm. This is consistent with freezing temperatures recorded in the literature.[12]

Once cooled to 173 K the diffraction patterns of the frozen droplets were measured between $2\theta = 19$ and 50°. Patterns are illustrated in Fig. 1b–g for a number of emulsion samples of varying droplet size. The peaks exclusive to ice I_h have been labelled "h" and the peaks common to both ice I_c and ice I_h have been labelled "h + c". Also shown for comparison is the diffraction pattern of pure ice I_h, generated by annealing pure water droplets at 263 K (Fig. 1a) and a diffraction pattern of ice I_c (Fig. 1h). Pattern 1h was obtained by freezing 45.2 wt% $(NH_4)_3H(SO_4)_2$ solution droplets, which froze between 192.4 ± 1 and 184.5 ± 1 K. This diffraction pattern is in very good agreement with the diffraction pattern of ice I_c reported in the literature.[1,3,4,13] Note that in the 45.2 wt% solutions, $(NH_4)_3H(SO_4)_2$ did not crystallize, and hence in the diffraction pattern only peaks due to ice are observed. The major ice I_h reflections at 34 and 44° are completely absent from this diffraction pattern, indicating the absence of bulk I_h. The peak at 23°, which is usually associated with the (100) reflection of ice I_h, is present in the diffraction pattern. This feature has been observed in previous studies of ice I_c employing X-ray diffraction[1,3,4,13] and neutron diffraction[14–16] and has been associated with hexagonal-like stacking faults, believed to be an intrinsic property of ice I_c.[3,14] Also, the region between 22 and 27° is raised above the background. This broad feature is also most likely related to stacking faults.[17,18]

Based on Fig. 1, the diffraction pattern of frozen water droplets with a volume median diameter of 5.6 μm (pattern g) has some similarities with the diffraction pattern for ice I_c with stacking faults (pattern h). First, the major ice I_h reflections at ~34 and 44° are significantly reduced in intensity relative to the peaks common to both ice I_h and ice I_c. Also, the region between $2\theta \approx 22.5$ and 26.5° is significantly raised above the background, similar to ice I_c with stacking faults.

As the volume median diameter was increased from 5.6 to 17.0 μm, the peaks exclusive to ice I_h increase in intensity relative to the peaks common to both ice I_c and ice I_h (see patterns b–g in Fig. 1). This indicates that there is a strong size dependence of the ice crystal structure with droplet size, and the amount of ice I_c decreases with an increase in droplet size. Overall, as the size increases, the diffraction pattern becomes more like the diffraction pattern of ice I_h.

The intensity ratios I_{44}/I_{40} and I_{33}/I_{47} (where I_{44} and I_{33} are the intensities of the exclusive hexagonal peaks at $2\theta \approx 43.5$ and 33.4°, and I_{40} and I_{47} are peak intensities common to cubic and hexagonal ice at $2\theta \approx 40.1$ and 47.1°) for the X-ray diffraction patterns illustrated in Fig. 1 have been plotted in Fig. 2 as a function of droplet size. These intensity ratios provide a convenient qualitative measure of the amount of ice I_h in the frozen droplets, where $I_{44}/I_{40} = 0.79 \pm 0.3$ and $I_{33}/I_{47} = 1.31 \pm 0.06$ indicates pure ice I_h and a value of zero indicates stacking faulty ice I_c (the ratios for pure hexagonal ice are determined from the hexagonal pattern illustrated in Fig. 1a).

The droplet diameter quoted in Fig. 1 and plotted in Fig. 2 is the volume median diameter (d_{vm}). The horizontal bars represent the particle diameter range over which 68% of the volume resides. These bars were calculated from the measured

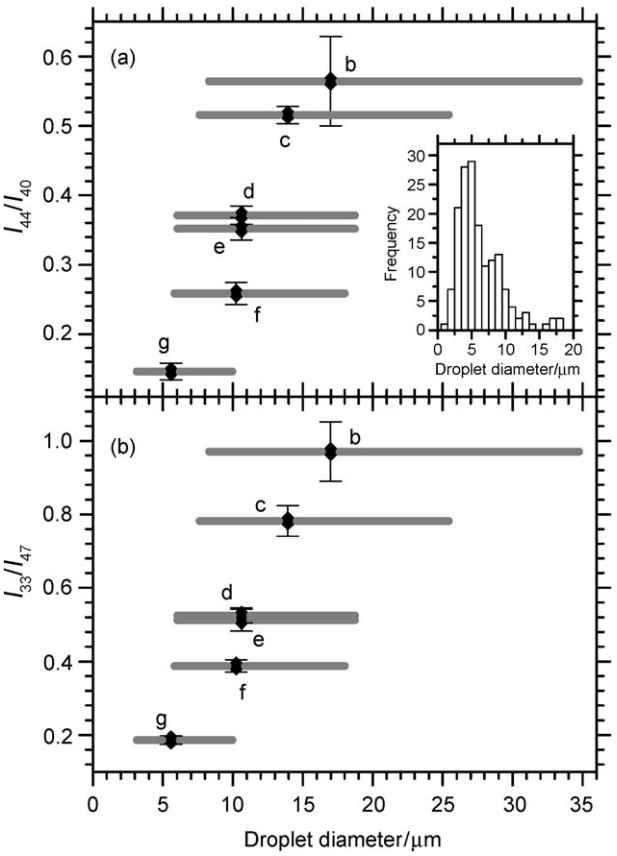

Fig. 2 The intensity ratio I_{44}/I_{40} (panel (a)) and I_{33}/I_{47} (panel (b)) as a function of the droplet volume median diameter (d_{vm}), which was determined from the measured droplet size distributions. A value of I_{44}/I_{40} or $I_{33}/I_{47} = 0$, indicates that no bulk ice I_h formed in the droplets, and therefore that the dominant product was ice I_c, whereas a value of $I_{44}/I_{40} = 0.79 \pm 0.03$ or $I_{33}/I_{47} = 1.31 \pm 0.06$ indicates pure ice I_h (these values were determined from the diffraction pattern of hexagonal ice illustrated in Fig. 1a). The horizontal bars represent the range of droplet sizes in which 68% of the volume resides. The vertical error bars are derived from the uncertainty associated with measuring the diffraction peak areas. The bracketed letters correspond to the diffraction patterns in Fig. 1. An example of a size distribution is shown as an insert; d_{vm} for these droplets was 10.6 μm with a geometric standard deviation of 1.8.

geometric standard deviation.[19] Fig. 2 illustrates the very strong dependence of the phase of ice on droplet size—as the size of the particles increases the amount of ice I_c decreases. When the volume median diameter is 5.6 μm, the droplets freeze close to pure ice I_c with stacking faults. Recently, based on classical thermodynamic calculations, it has been suggested that pure water droplets smaller than 30 nm in diameter would freeze to cubic ice and bigger droplets would freeze to hexagonal ice.[20] These calculations do not agree with our observations that water droplets with a volume median diameter of 5.6 μm freezes dominantly to ice I_c.

The decrease in the amount of ice I_c as the size is increased from 5.6 μm can be explained with heat transfer calculations. When a water droplet freezes heat is produced, since crystallization is an exothermic process. If the heat is not dissipated

to the droplet's environment more rapidly than it is produced during crystallization, the temperature of the droplet will increase during freezing, which can allow ice I_c regions in the ice droplet to anneal to ice I_h (it will be shown later in this paper that the ice I_c to ice I_h transition occurs more readily at higher temperatures). Based on equations given in Pruppacher and Klett,[12] and temperatures and thermal properties consistent with our experiments, a droplet of 10 μm in diameter will dissipate heat to the oil matrix at a rate similar to the rate of heat production within the supercooled droplet due to crystallization. As a result 10 μm particles may not warm up sufficiently to anneal all ice I_c to ice I_h, which is consistent with our experimental results. Smaller droplets will have a greater surface area to volume ratio than larger droplets and will therefore dissipate heat more efficiently. Hence, one would expect the amount that the particle warms up, and therefore the amount of ice I_c, to depend strongly on droplet size, which is in agreement with our observations. Our combined results are consistent with ice I_c nucleating in all of the droplets, and the final amount of ice I_c being governed by the amount the temperature of the droplet increases during freezing. From this we infer that ice I_c, rather than ice I_h, is likely to be the crystalline phase that nucleates when water droplets freeze homogeneously at ~235 K. In making this statement, we assume that the crystalline phase of the ice nucleus is the same as the crystalline phase observed in the small droplets, which experience no appreciable heating. This is similar to assumptions that have been previously made in the literature.[5] This also assumes that crystallization begins with the formation of a critical nucleus with a well defined crystal structure, which is still a matter of debate in the literature.[21]

Our inference that homogeneous nucleation of water droplets at ~235 K begins with ice I_c is consistent with thermodynamic arguments that indicate the free energy of formation of an octahedral germ of ice I_c is lower than the free energy of formation of an ice I_h germ.[8,22] Also these results are consistent with previous experiments by Huang and Bartell.[5] These authors froze water clusters (5.5–6.6 nm) at 200 K in a supersonic expansion and determined the free energy of the solid–liquid interface when ice nucleated in these clusters. They found that the clusters froze to ice I_c, using electron diffraction, and they also noticed that the interfacial energies they determined were consistent with those determined from homogeneous freezing experiments of emulsified water droplets. Based on this they concluded that ice I_c initially nucleates in water droplets at ~235 K as well as at 200 K. Furthermore, it has been suggested that ice I_c is the phase that nucleates based on measurements of the angles between the *c*-axis in snow polycrystals and frozen water droplets.[6,7] These previous measurements combined with our direct measurements of the phase of ice that forms in water droplets provides convincing evidence that ice I_c is the crystalline phase that nucleates when pure water droplets freeze homogeneously at ~235 K.

In Fig. 3, we have compared experimental diffraction patterns of frozen water droplets with composite patterns generated by taking a linear combination of the pattern of pure ice I_h (Fig. 1a) and ice I_c with stacking faults (Fig. 1h). The best fits were determined by minimizing the sum of squares differences between the experimental and composite patterns. The agreement between measured and composite patterns (open circles and solid lines, respectively) is good. The good agreement suggests that pure water droplets may freeze to a combination of ice I_h and stacking faulty ice I_c. The proportions of ice I_c with stacking faults and ice I_h determined from this analysis have been quoted in Fig. 3. This analysis has also been applied to the other diffraction patterns in Fig. 1, and the proportions of stacking faulty ice I_c from this analysis are also quoted there. When estimating the proportion of stacking faulty ice I_c and ice I_h it was assumed that the X-ray quantitation constants (integrated intensity per unit mass of ice) for the common peaks are the same for hexagonal ice and cubic ice

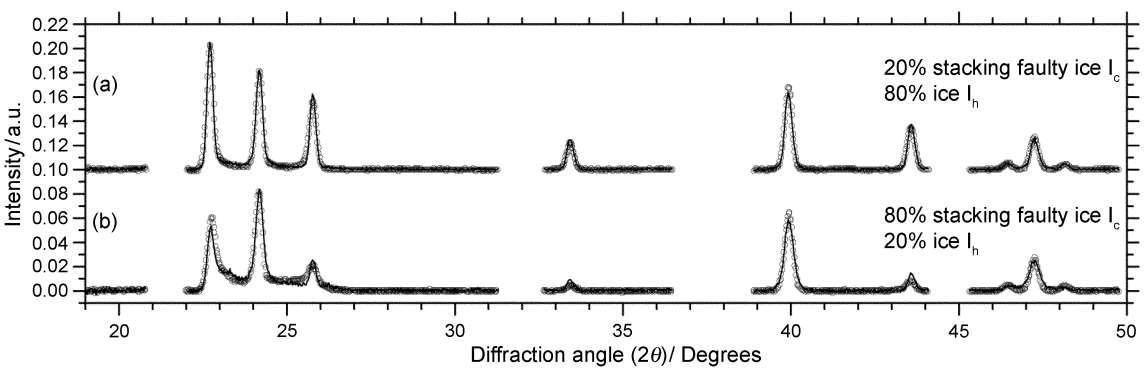

Fig. 3 Comparison of composite (solid lines) and measured X-ray diffraction patterns (points). The composite patterns result from a linear combination of two separate patterns: the first is a pattern of 45.2 wt% $(NH_4)_3H(SO_4)_2$ solution droplets which froze at around 188 K to stacking faulty ice I_c (illustrated in Fig. 1h); the second diffraction pattern (illustrated in Fig. 1a) is that of pure water which froze around 235 K and was subsequently annealed at 263 K to form ice I_h with no detectable stacking faults or regions of ice I_c. The pure ice I_h pattern and the stacking faulty ice I_c pattern were scaled and added together to give the composite patterns. The scaling factors were determined by minimizing the sum of squares differences between the composite and experimental patterns and the resulting proportions of stacking faulty cubic ice and hexagonal ice are indicated in the figure (assumptions and uncertainties associated with these values are discussed in the text). The measured patterns are (a) droplets of d_{vm} = 13.9 μm (Fig. 1c) and (b) droplets of d_{vm} = 5.6 μm (Fig. 1g). All patterns were background subtracted. The regions of the diffraction patterns influenced by diffraction from the cell construction materials were not included when calculating the sum of squares differences and have been removed for clarity.

with stacking faults. Measurements in which we monitor the intensity of the common peaks as cubic ice with stacking faults is annealed to hexagonal ice show that the X-ray quantitation constants are the same to within 5%. Note that the quantitation constants of the common peaks for pure cubic ice (samples free of stacking faults) will be different from the quantitation constants for hexagonal ice, based on calculations of the diffraction patterns using the POWDER CELL programme.[10] Evidently stacking faults appear to influence the quantitation constants of cubic ice. Assuming a 10% uncertainty in quantitation constants, the proportions of stacking faulty ice I_c and ice I_h only change by at most 5%.

In the future we will carry out a full modelling study of the diffraction patterns to quantitatively evaluate the proportions of ice I_c and ice I_h as well as investigate the nature and density of stacking faults. Further experiments are also required to determine if individual frozen droplets contain regions of ice I_h and ice I_c with stacking faults or if individual droplets freeze exclusively to a stacking faulty cubic structure or a hexagonal structure.

The stability of ice I_c in water–oil emulsions (*i.e.* the transformation of ice I_c to ice I_h in frozen water droplets suspended in an oil matrix).

In this series of experiments the transformation of the ice I_c component of the frozen pure water droplets was investigated as a function of time at several temperatures between 228 and 263 K. Emulsified droplets of $d_{vm} \approx 10$ μm were cooled at a rate of 10 K min^{-1} to 223 K, and then the temperature was rapidly ramped to the temperature of the isothermal transformation measurement (T_{trans}). While the frozen droplets were held at $T_{trans} \pm 0.2$ K, the diffraction pattern between $2\theta = 39.3$ and 44.3° was monitored. This covers the exclusive ice I_h reflection at $2\theta \approx 43.5°$ and the reflection common to both ice I_c and ice I_h at $2\theta \approx 40°$.

The ratio I_{44}/I_{40} determined during the isothermal transformation measurements is plotted in Fig. 4. Prior to starting the isothermal transformation measurements I_{44}/I_{40} was close to 0.4 in all measurements, which indicates that a significant amount of ice I_c resulted from the freezing process, as expected from the earlier work. The results in Fig. 4 show that at 228 K ice I_c is very stable. When the ice was held at 228 K the frozen droplets still contained a significant amount at ice I_c after nearly 12 h, with an intensity ratio $I_{44}/I_{40} = 0.56 \pm 0.02$ (recall that I_{44}/I_{40} for stacking faulty ice I_c is 0 and for pure ice I_h it is 0.79 ± 0.03). In fact, even after nearly 5 h at 238 K the ice had not fully relaxed to perfect ice I_h ($I_{44}/I_{40} = 0.65 \pm 0.03$). In contrast ice I_c at 263 K is rapidly converted to ice I_h, and at 243 K, almost all of the ice I_c is converted to ice I_h ($I_{44}/I_{40} = 0.73 \pm 0.05$) after 178 min.

To test if X-ray exposure was influencing the ice films during the annealing experiments, we repeated the measurements at 228 K, but this time the shutter to the X-ray source was only opened for enough time to establish the ratio I_{44}/I_{40} once every few hours. The results of this test (not shown) are in agreement within the uncertainty of the measurement with the results presented in Fig. 4 (open triangles) indicating that the exposure to X-rays did not significantly affect the ice crystal structure.

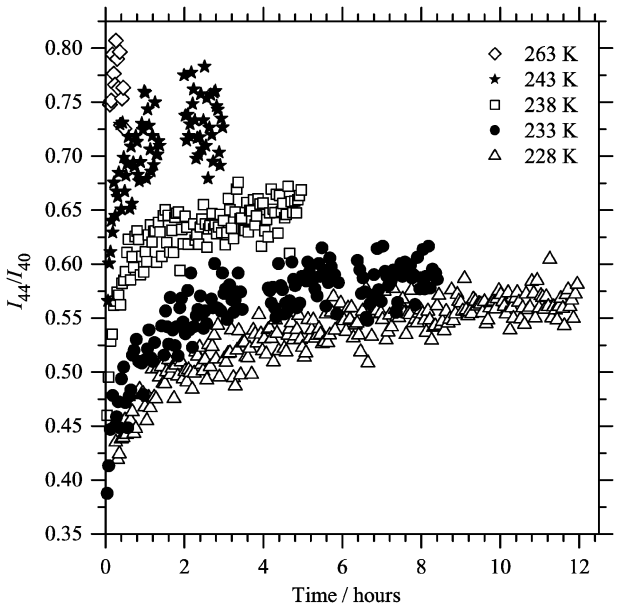

Fig. 4 The intensity ratio I_{44}/I_{40} as a function of time after freezing for pure water droplets ($d_{vm} \approx 10$ μm). A value of 0.79 ± 0.3 corresponds to the ratio of ice I_h with no detectable ice I_c stacking faults, and a value of zero indicates that no bulk ice I_h formed in the droplets, and therefore that the dominant product was ice I_c. Results are shown for several different isothermal transformation temperatures.

Many of the previous measurements of the ice I_c to ice I_h phase transition have found that ice I_c transforms to ice I_h rapidly below ~205 K.[23] It has been suggested that the ice I_c to ice I_h phase transition is related to surface area —very high surface area ice I_c tends to transform more rapidly and at lower temperatures to the stable ice I_h.[4] In high surface area ice I_c samples, surface nucleation is likely to be much more rapid[4] and also possibly mass transfer from ice I_c crystals to ice I_h crystals *via* the gas phase may have dominated in many experiments.[2] In our experiments the particles are suspended in an oil matrix and hence mass transfer *via* the gas phase and possibly surface nucleation were blocked, which provides an explanation for the longer lifetimes at higher temperatures observed in our studies.

Our long lifetimes at higher temperatures are consistent with a number of studies of low surface area ice I_c. Using X-ray diffraction Mayer and Hallbrucker[4] found that ice I_c samples, prepared by hyperquenching water droplets, required around 30 min at 240 K to fully convert to ice I_h. Using a similar technique to produce ice I_c, Kohl *et al.*[3] found that the transition was centred around 230 K, while Kuhs *et al.*[15] found that a sample of ice I_c made from ice V mostly transformed below 205 K, but a significant portion remained in the cubic phase up to between 237 and 245 K. Kuhs *et al.* suggested this cubic portion of their ice took the form of planar stacking faults within ice I_h. Cubic ice has also been observed at higher temperatures in porous silica.[24] The stability in these experiments is likely due in part to the confined geometries.

Also of interest is the nonlinear trend observed in Fig. 4. For example, at 233 K there is a fast increase in the ratio and then it levels off, indicating that a certain fraction of the cubic ice is very long lived. This is consistent with the measurements of Kuhs *et al.*,[15] described above in that portions of the ice I_c appear to be more stable than others. The fact that a similar trend was observed using two very different methods of preparing ice I_c suggests that this trend may be an intrinsic property of cubic ice. Possibly related, Johari argued that ice I_c and I_h can coexist over a broad temperature range due to contributions from grain boundaries, interphases and strain energies.[25] The nonlinear trend observed in Fig. 4 may also be related to slow nucleation kinetics in some frozen droplets. As mentioned we most likely only measured the solid state transition (as the vapour-mediated transformation is blocked). Therefore, the phase transition is likely initiated by nucleation in lattice imperfections, such as line defects and at grain boundaries.[26] Some frozen droplets may have significantly less imperfections for nucleation of ice I_h, resulting in some frozen droplets with very long lived ice I_c regions. Smaller frozen particles may have significantly less imperfections compared to large particles, assuming the occurrence of imperfections is random. In this case, ice I_c in the smaller particles will be more stable than in the larger particles (assuming the conversion rate is limited by nucleation at lattice imperfections). Further research is needed on this topic.

Conclusions

The data presented in this paper are consistent with the emulsified water droplets freezing to a significant proportion of stacking faulty ice I_c and that the proportion of stacking faulty ice I_c increases as the droplets decrease in size. In fact, droplets of volume median diameter 5.6 μm appear to freeze dominantly to ice I_c with stacking faults. The size dependence can be rationalised with heat transfer calculations since smaller droplets, with a large surface area to volume ratio, will dissipate heat more rapidly and be less likely to form ice I_h. These results support previous suggestions that ice I_c is the crystalline phase that nucleates when pure water droplets freeze homogeneously at ~235 K.[5–9]

When water droplets freeze in the atmosphere, our results suggest that ice I_c will initially nucleate. However, heat transfer calculations show that when droplets freeze in the atmosphere they will be more likely to freeze to ice I_h than droplets in our emulsion experiments. The rate of heat dissipation for a particle suspended in a gas will be roughly a factor of 10 smaller for a similar droplet suspended in oil due to the difference in thermal conductivity of the medium.[27] According to simple heat transfer calculations,[12] a 1 μm droplet in the atmosphere will have a similar propensity for freezing to ice I_c as a 10 μm droplet in our experiment. Heymsfield and Miloshevich[28] found evidence that liquid droplets smaller than 3 μm froze homogeneously below 237 K in orographic wave clouds; we suggest that these droplets may have frozen to a significant amount of ice I_c.

We observe ice I_c up to 243 K, much higher in temperature than observed in many previous studies.[23] This result adds to the existing literature[3,4,15] that shows ice I_c can persist up to ~240 K. Our results focus on the solid state transformation since we most likely blocked surface nucleation and vapour transport by placing droplets in an oil emulsion in contrast to most previous studies.

The ice I_c to ice I_h measurements show a complex time and temperature dependence of the phase transition. The transformation proceeds rapidly at first and then slows down and comes to a halt. This could be because a fraction of the frozen droplets have fewer lattice imperfections and hence the ice I_c in these particles is more stable. Alternatively, the results may in part be due to ice I_c stacking sequences that persist at temperatures above 205 K.[15]

The results from this study, combined with results from other studies, help explain why ice I_c is observed in some bulk samples and not others: Ice I_c must always be held below ~240 K regardless of the surface area of the sample or else it will be rapidly converted to ice I_h through a solid state tranformation. (One exception is ice I_c formed in nanoporous material, which can exist to higher temperatures, possibly due to the confined geometries.[24]) Also, during the crystallization process, the rate of heat dissipation from the sample needs to be greater than the rate of heat production by crystallization or else the sample will heat up and the ice I_c may be converted to ice I_h. In addition, if the ice has a high surface area and mass transfer *via* the vapour is not blocked, it must be prepared below ~200 K, or else surface nucleation and mass transfer will occur and any ice I_c that forms will be converted rapidly to ice I_h, by vapour-mediated transformation. This overall discussion is consistent with our measurements as well as most measurements of ice I_c reported in the literature.[3,4,13,23]

Acknowledgements

We thank A. Lam and B. Patrick for their assistance with the X-ray diffraction measurements and the interpretation of the diffraction patterns and R. Signorell for helpful comments on the manuscript. This work was funded by the Canadian Foundation for Climate and Atmospheric Sciences, CFCAS, the Natural Science and Engineering Research Council of Canada, NSERC, the Canada Foundation for Innovation, CFI, and the Canada Research Chairs Program.

References

1 B. J. Murray, D. A. Knopf and A. K. Bertram, *Nature*, 2005, **434**, 202–205.
2 D. M. Murphy, *Geophys. Res. Lett.*, 2003, **30**.
3 I. Kohl, E. Mayer and A. Hallbrucker, *Phys. Chem. Chem. Phys.*, 2000, **2**, 1579–1586.
4 E. Mayer and A. Hallbrucker, *Nature*, 1987, **325**, 601–602.
5 J. F. Huang and L. S. Bartell, *J. Phys. Chem.*, 1995, **99**, 3924–3931.
6 Y. Furukawa, *J. Met. Soc. Japan*, 1982, **60**, 535–547.
7 T. Takahashi and T. Kobayashi, *J. Cryst. Growth*, 1983, **64**, 593–603.
8 H. Kiefte, M. J. Clouter and E. Whalley, *J. Chem. Phys.*, 1984, **81**, 1419–1420.
9 L. S. Bartell and Y. G. Chushak, in *Water in Confined Geometries*, ed. V. Buch and J. P. Devlin, Springer-Verlag, Berlin, 2003, pp. 399–424.
10 W. Kraus and G. Nolze, *J. Appl. Crystallogr.*, 1996, **29**, 301–303.
11 A. Goto, T. Hondoh and S. Mae, *J. Chem. Phys.*, 1990, **93**, 1412–1417.

12 H. R. Pruppacher and J. D. Klett, *Microphysics of Clouds and Precipitation*, Kluwer, Dordrecht, 1997.
13 L. G. Dowell and A. P. Rinfret, *Nature*, 1960, **188**, 1144–1148.
14 W. F. Kuhs, D. V. Bliss and J. L. Finney, *J. Phys. Colloq.*, 1987, **48**, 631–636.
15 W. F. Kuhs, G. Genov, D. K. Staykova and T. Hansen, *Phys. Chem. Chem. Phys.*, 2004, **6**, 4917–4920.
16 G. P. Arnold, E. D. Finch, S. Rabideau, W. and R. G. Wenzel, *J. Chem. Phys.*, 1968, **49**, 4365–4369.
17 A. I. Ustinov, in *Defect and Microstructure Analysis by Diffraction*, ed. R. Snyder, J. Fiala and H. J. Bunge, Oxford University Press, Oxford, 1999, pp. 264–317.
18 Z. Weiss and P. Čapková, in *Defect and Microstructure Analysis by Diffraction*, ed. R. Snyder, J. Fiala and H. J. Bunge, Oxford University Press, Oxford, 1999, pp. 318–329.
19 P. C. Reist, *Aerosol Science and Technology*, McGraw-Hill, New York, 1993.
20 G. P. Johari, *J. Chem. Phys.*, 2005, 122.
21 M. Matsumoto, S. Saito and I. Ohmine, *Nature*, 2002, **416**, 409–413.
22 T. Takahashi, *J. Cryst. Growth*, 1982, **59**, 441–449.
23 P. Hobbs, *Ice Physics*, Oxford University Press, London, 1974.
24 D. C. Steytler, J. C. Dore and C. J. Wright, *J. Phys. Chem.*, 1983, **87**, 2458–2459.
25 G. P. Johari, *Philos. Mag. B*, 1998, **78**, 375–383.
26 Y. V. Mnyukh and N. A. Panfilova, *J. Phys. Chem. Solids*, 1973, **34**, 159–170.
27 R. C. Weast, *Handbook of Physics and Chemistry*, CRC Press, Boca Raton, 70th edn, 1990.
28 A. J. Heymsfield and L. M. Miloshevich, *J. Atmos. Sci.*, 1993, **50**, 2335–2353.

